REST Journal on Emerging trends in Modelling and Manufacturing
Vol:2(1),2016
REST Publisher
ISSN: 2455-4537

Website: www.restpublisher.com/journals/jemm

Effect of Geometry and Array of Cooling Holes in Film Cooling Over an Adiabatic Flat Plate – A Computational Approach

Madhurima Dey[1], Prakhar Jindal[2] and A.K. Roy[3], Kaushik Kumar[4†]
[1,2] Research Scholar, Birla Institute of Technology, Mesra, Ranchi, Jharkhand, 835215, India
[3,4]Associate Professor, Birla Institute of Technology, Mesra, Ranchi, Jharkhand, 835215, India
†Corresponding Author Email: kkumar@bitmesra.ac.in

Abstract

Computational analysis has been carried out to find the film cooling effectiveness (centerline and spatially averaged) over an adiabatic flat plate. Variation in film cooling effectiveness has been determined along the downstream of the cooling holes on the flat plate. The study compares film cooling effectiveness over various blowing ratios, various hole shapes and rearrangement of holes. Here three different cooling hole shapes i.e. circular, square and fan shaped holes have been used for the present study. Numerical based solver Fluent has been used for the analysis using the standard Reynolds Averaged Navier-Stokes shear stress transport turbulence model. The numerical results reveal that the film cooling effectiveness increases with increase in blowing ratios. Beyond an optimum blowing ratio, film cooling effectiveness decreases due to coolant jet lift off and intermixing of coolant and mainstream flow at higher blowing ratio. Among the different cooling hole shapes, the best film cooling effectiveness was obtained for fan-shaped holes with blowing ratio equal to unity. Spatially averaged effectiveness for fan-shaped holes was found to be higher as compared to other hole shapes.

Keywords: blowing ratio, fan-shaped hole, spatially averaged effectiveness, film cooling effectiveness.

NOMENCLATURE

D	diameter
k	turbulent kinetic energy
M	blowing ratio
T_{aw}	adiabatic wall temperature
T_c	coolant temperature
T_∞	mainstream temperature
x/D	position at x-axis to diameter ratio
y/D	position at y-axis to diameter ratio
ε	turbulence dissipation
η	film cooling effectiveness
ω	specific dissipation rate

I. Introduction

Adiabatic plate is very common which finds application in gas turbine blades, combustion chamber walls etc. Modern gas turbines encounter very high operating fluid temperatures which may result in damaged turbine blades. In order to prevent failure of turbine blades resulting from these excessive operating fluid temperatures, a comprehensive cooling technique known as film cooling can be incorporated during blade designing process. To maintain the balance between excessive heating and excessive cooling of the turbine blades an optimum cooling technique is highly desired. Film cooling effectiveness is a non-dimensional parameter used to characterize the film cooling performance. Mathematically, Film cooling effectiveness [1] is defined as:

$$\eta = \frac{(T_\infty - T_{aw})}{(T_\infty - T_C)} \qquad (1)$$

Many experimental and computational works have been performed by various researchers. Some literatures which are relevant to present work are given here. Kadja and Bergelest [1] used two dimensional numerical model and found that effective blade surface cooling is possible when blowing ratio (M) is increass but cycle efficiency reduces. Michael [2] presented detailed measurements of local heat transfer coefficient in the vicinity of cooling holes with different hole geometries. Garg [3] used Wilcox's k-ω model and found that coolant velocity and temperature distribution at hole exits do not follow $1/7^{th}$ Power Law and are highly skewed by mainstream flow. He has observed that distribution of k and ω at exit of holes are also skewed. Lee et al. [4] found occurrence of reverse flow from mainstream to film hole at hole exit plane for orientation angle as 60^0. Yuen and Botas[5] studied effectiveness of film cooling characteristics of a single round hole at various streamwise angles in a crossflow. Ahn et al. [6] studied the interaction between the coolant and mainstream. They have observed that in inline configuration coolant is well attached to wall with the help of downwash flow formed at the hole exit implying high effectiveness (η) whereas upwash flow deteriorates it. They have concluded that lower blowing ratio (M) = 0.5 provides highest η in near hole area whereas higher M gives better protection in the farther downstream

area. Mayhew et al. [7] experimentally predicted high free stream turbulence at high M increase the area averaged η and low M decrease the area averaged η due to increase in intermixing of coolant with main flow. Tao et al. [8] carried out numerical simulation as well as experimental investigation to find out effectiveness for a rotating blade . They have concluded that the standard k-ε model gave poor results whereas the k-ω and SST k-ω turbulence model gave relatively better results and produced closer estimation for pressure side and suction side due to isotropic characteristics. Vickery and Iacovides [9] computationally determined that maximum effectiveness occur at some distance downstream of the hole and zero η at mid span between a pair of injection holes. They have observed that higher turbulence levels lead to an increase in the coolant and free stream interactions and therefore a reduction in the effectiveness. Vickery and Iacovides [9] found that high density ratio of coolant (D.R) result in improved lateral spread of flow downstream of injection holes improving the effectiveness. Kim et al. [10] did comparative analysis on various shapes of film cooling holes. They found that dumbbell-shaped hole shows the best spatially averaged film-cooling effectiveness for all blowing ratios. Elnady et al. [11] did experimental investigation to improve film cooling performance on the leading edge of a gas-turbine vane. They found that cooling effectiveness improved with increase in blowing ratio due to the jet lift-off reduction and hence higher cooling capacity is achieved. Raj and K. [12] performed computational work and found that as blowing ratio increases, the local stream-wise effectiveness increases and causes coolant jet lift off. They also found that boundary layer developed in the wall jet region is removed due to suction created by film cooling holes and thus increasing heat transfer. The reattachment of coolant in the flow structure increases the effectiveness near the leading edge of the holes. Vidit Sharma and Ashish Garg [13] studied on effects of compound angle and length to diameter ratio on adiabatic film cooling effectiveness. They found that laterally averaged adiabatic effectiveness is the function of length to diameter ratio and compound angle. Jindal et al. [14] studied on film cooling effectiveness and heat transfer on a three dimensional flat plate with a cylindrical, elliptic and triangular holes having an inclination of 30^0. It was found that triangular hole shows higher effectiveness than cylindrical hole in the near hole area. It was also observed that triangular hole shows less coolant jet height and high film cooling effectiveness at higher blowing ratios. From the above literatures it can be concluded that film cooling effectiveness depend on various parameters such as wall geometry, wall curvature, boundary layer influence, coolant velocity, free stream turbulence, momentum flux ratio, injection angle, free stream Mach number, viscosity of coolant, etc. The main objective of this paper is to analyze the film cooling effectiveness on an adiabatic flat plate using the SST k-ω turbulence model as suggested by Tao et al. [8] using FLUENT solver. The 3-D model of the present work and meshed model have been made using GAMBIT. Comparison have been for film cooling effectiveness on various blowing ratios (M = 0.60, 0.83 and 1.00) for different hole geometries and arrangement of hole shapes.

II. Modelling of The present work

A. Geometry

A schematic view of the model for the present work for a circular shaped cooling hole is shown in Fig. 1(a). Fig. 1(b) shows the side view of the model (computational model) with dimensions. The geometry of the circular and square hole shapes at the inlet and out let is circular and square respectively. While for the case of fan-shaped hole, it is circular at inlet and fan-shaped at the outlet to ease the manufacturability. In case of fan-shaped hole, the exit area is thrice the entry area which has been found out from the work of Michael Gritsch et al. [2] since fan-shaped are categorized as expanded exits. In this work single hole and shower hole arrangement have been considered for the present study. It is to be noted that the volume of three kinds of holes has been kept constant and which is equal to 1963.5 mm^3. The volume of all the hole shapes has been kept constant so as to compare the results based on constant coolant mass flow rate from each hole. The geometrical shape and size of the cooling holes are tabulated in Table 1.

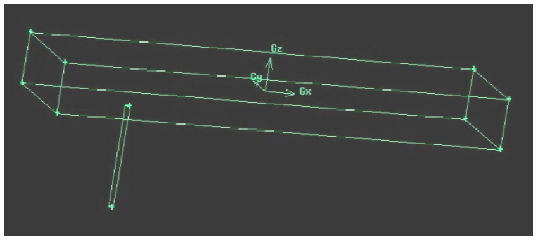

Fig. 1(a). Model of the Present Work (single hole)

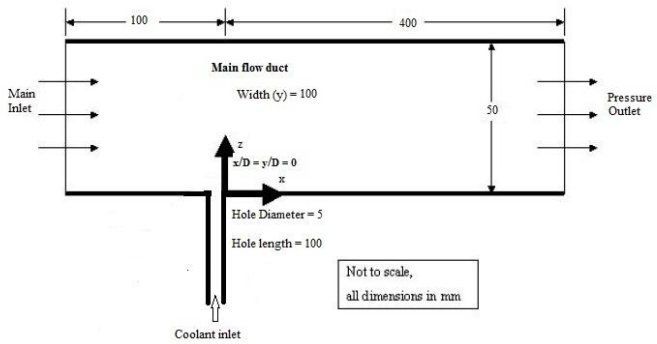

Fig. 1(b). Side View of the Computational Model (single hole)

Table 1 Geometric Shape and Size of Cooling Holes

Types of holes	Inlet cross section	Outlet cross section	Volume of the hole
Circular hole inlet with circular hole outlet	19.635mm^2	19.635mm^2	1963.5 mm^3
Square hole inlet with square hole outlet	19.635mm^2	19.635mm^2	1963.5 mm^3
Circular hole inlet with fan shaped hole outlet	19.635mm^2	58.89 mm^2	1963.5 mm^3

B. *Boundary Condition & Governing Equations*

Boundary condition which has been set in the model is shown in Table 2.

TABLE 2 Boundary Condition

Main inlet	Velocity Inlet
Main outlet	Pressure Outlet
Lower Wall	Interface
Upper Wall	Wall
Side Walls	Wall
Coolant Inlet	Velocity Inlet
Coolant Outlet	Interface
Coolant Wall	Wall
Coolant and main stream material	Air

At the main inlet, a velocity-inlet boundary condition has been specified with x-velocity equal to 25 m/s. The mainstream and coolant temperatures are 600K and 300K respectively. The coolant injection angle is 90^0 as shown in Fig. 1(b). The ratio of coolant to mainstream mass flux is defined as blowing ratio (M). Table 3 shows the corresponding coolant velocity used according to different blowing ratios.

$$M = \frac{\rho_c U_c}{\rho_\infty U_\infty} \tag{2}$$

TABLE 3 Blowing Ratios and Coolant Inlet Velocities

Sl No.	Blowing Ratios (M)	Coolant Velocities (m/s)
01.	0.60	15.00
02.	0.83	20.75
03.	1.00	25.00

For a fluid, with constant thermo-physical properties, the governing equations for turbulent, steady flow as stated by Kadja and Bergelest [1] are as follows.

Continuity equation;

$$\frac{\partial \rho U_1}{\partial x_1} = 0 \tag{3}$$

Momentum equations;

$$\frac{\partial \rho U_j U_i}{\partial x_j} = -\frac{\partial P}{\partial x_i} + \frac{\partial}{\partial x_j}\left[(\mu + \mu_\tau)\left(\frac{\partial U_i}{\partial x_j} + \frac{\partial U_j}{\partial x_i}\right)\right] \tag{4}$$

Energy equation;

$$\frac{\partial \rho U_i \theta}{\partial x_j} = \frac{\partial}{\partial x_j}\left[(\gamma + \gamma_\tau)\frac{\partial \theta}{\partial x_j}\right] \tag{5}$$

Turbulent kinetic energy equation;

$$\frac{\partial \rho U_i k}{\partial x_j} = \mu_\tau\left(\frac{\partial U_i}{\partial x_j} + \frac{\partial U_j}{\partial x_i}\right)\frac{\partial U_i}{\partial x_j} + \frac{\partial}{\partial x_j}\left(\frac{\mu_\tau \partial k}{\sigma_k \partial x_j}\right) - \rho\varepsilon \tag{6}$$

Rate of dissipation of turbulent kinetic energy equation;

$$\frac{\partial \rho U_j \varepsilon}{\partial x_j} = \mu_\tau C_1 \frac{\varepsilon}{k}\left(\frac{\partial U_i}{\partial x_j} + \frac{\partial U_j}{\partial x_i}\right)\frac{\partial U_i}{\partial x_j} + \frac{\partial}{\partial x_j}\left(\frac{\mu_\tau \partial \varepsilon}{\sigma_\varepsilon \partial x_j}\right) - \rho C_2 \frac{\varepsilon^2}{k} \tag{7}$$

where μ_τ is the turbulent viscosity; the density ρ is obtained from the ideal gas equation of state P = ρrΘ , *r* being the gas constant (in this case air); γ is the thermal diffusivity, λ is the thermal conductivity and C_P the specific heat at constant pressure) and γ_τ the turbulent thermal diffusivity. The constants of the Standard k-ω model used are: $C_1 = 1.44$; $C_2 = 1.92$;

$\sigma_k = 1.0;\ \sigma_\varepsilon = 1.3$

C. *Validation and Grid independency test*

The computational model has been validated with benchmark experimental literature [5] for a circular hole case at M = 0.60 as shown in Fig. 2. The computational results almost matches with the experimental result obtained by Yuen and Botas [5] while experimenting on a cylindrical hole with a streamwise angle of 30^0, 60^0 and 90^0.

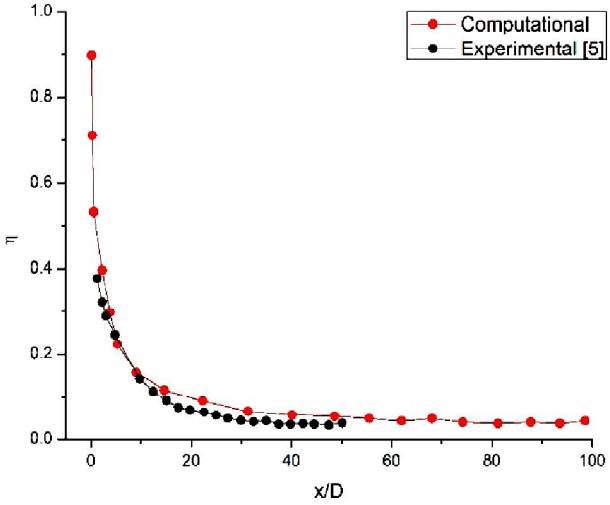

Fig. 2. Effectiveness for Circular Hole at Blowing Ratio M = 0.60

The grid independency test have been carried out for M = 0.60. The meshes were created using Gambit. Fig. 3 shows meshed geometrical model with 32, 50,000 hexahedral cells made using copper scheme [5]. Mesh for circular and fan-shaped holes consist of 28, 38,225 and 25, 65,000 hexahedral cells respectively. From Fig. 4, it is concluded that the medium grid gave almost similar comparison to published experimental results and thus have been used for subsequent computations. Hybrid geometry was used for interface.

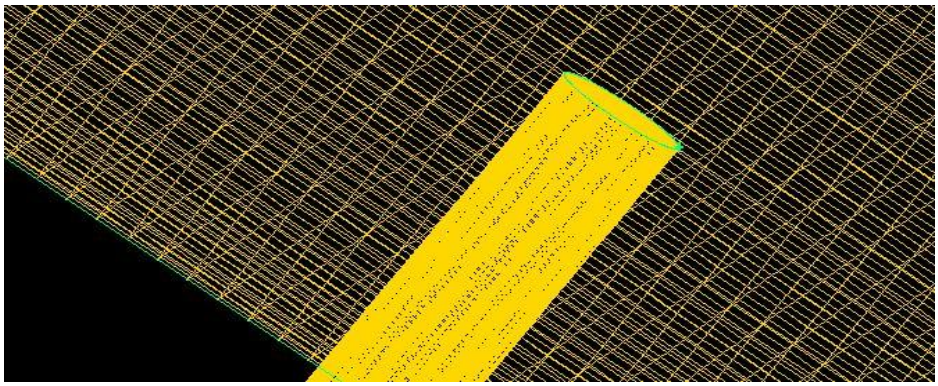

Fig. 3. Meshed Geometrical Model near Wall

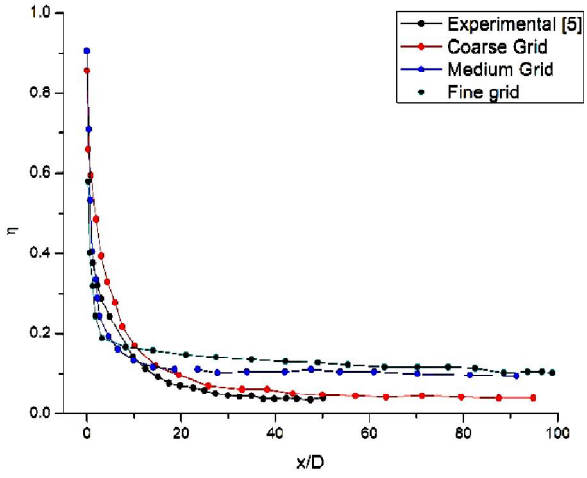

Fig. 4. Grid Independency Test

D. *Solver*

The simulation has been carried out using RANS shear stress transport model in FLUENT. The k-ω SST model has been used because it makes the model directly usable at the wall through the viscous sub-layer as found out by Tao et al. [8] and Raj and K. [10]. Hence, the k-ω SST model has been used as a Low-Re turbulence model without any extra damping functions. The SST formulation also switches to a k-ε behavior in the free-stream and thereby avoids the common k-ω problem that the model is too sensitive to the inlet free-stream turbulence properties. The SST k-ω model show good behavior in adverse pressure gradients and separating flow. This model produces large turbulence levels in regions with large normal strain, like stagnation regions and regions with strong acceleration.

III. Results and Discussions

A. *Variation of Centerline Effectiveness at Different Blowing Ratios (Single Hole)*

Figs. (5- 7) show comparison of centerline effectiveness for single circular, square and fan-shaped hole at an axial distance of 400 mm from the leading edge of the blade for M = 0.60, 0.83 and 1 respectively. Fig. 5(a) shows configuration of a single circular hole and Fig. 5(b) shows centerline effectiveness of it at different blowing ratios. Fig. 6(a) shows configuration of a single square hole and Fig. 6(b) shows centerline effectiveness of it at different blowing ratios. Fig. 7(a) shows configuration of a single fan-shaped hole and Fig. 7(b) shows centerline effectiveness of it at different blowing ratios. From Figs.(5-7) it can be observed that as blowing ratio increases from 0.60 to 1.00, film cooling effectiveness increases at coolant exit but reduces further downstream of circular and square shaped holes due to rapid increase in intermixing of coolant and mainstream flow. Effectiveness at coolant exit for square hole case is less than circular hole due to presence of lateral separation of kidney vortices. Hence, at exit only coolant spread more laterally whereas in circular hole case coolant could not spread and cover narrow area. In fan-shaped hole, film cooling effectiveness is minimum at hole exit due to coolant jet lift off. Then, coolant jet reattachment takes place and effectiveness almost approaches to unity. As blowing ratio increases from 0.60 to 1.00 effectiveness also increases at coolant exit as well as further downstream of cooling hole.

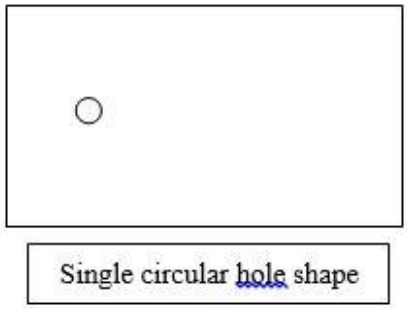

Fig. 5(a). Configuration for Circular Hole,

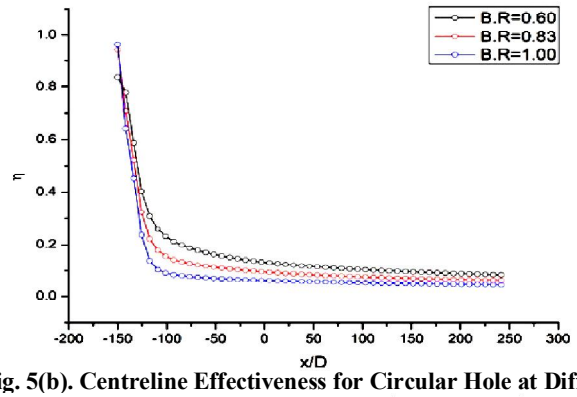

Fig. 5(b). Centreline Effectiveness for Circular Hole at Different M

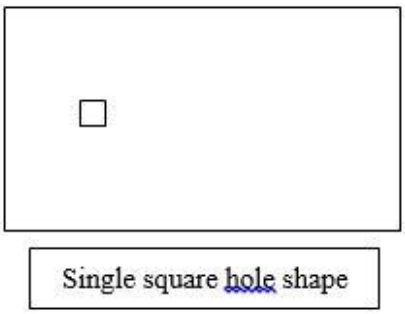

Fig. 6(a). Configuration for Square Hole,

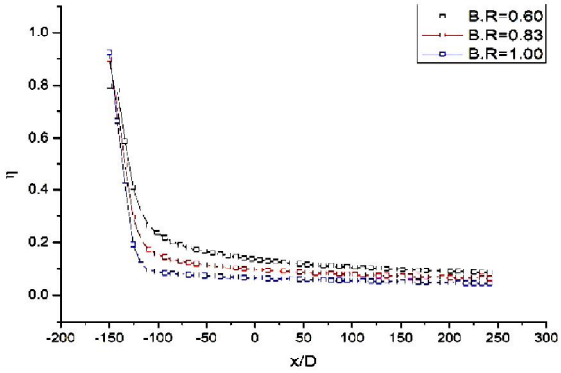

Fig. 6(b). Centreline Effectiveness for Square Hole at Different M

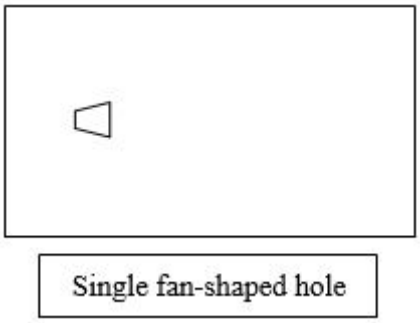

Fig. 7(a). Configuration for Fan-Shaped Hole,

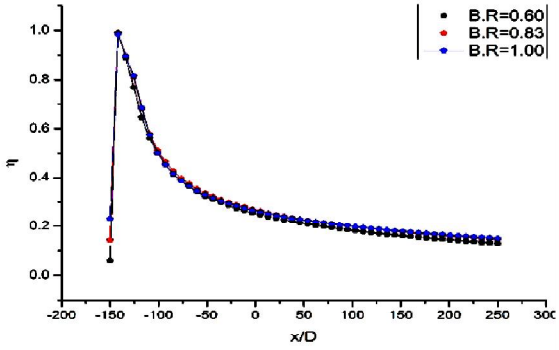

Fig. 7(b). Centerline Effectiveness for Fan-Shaped Hole at Different M

Fig. 8 shows comparison of centerline effectiveness for different hole shapes at M = 0.60, 0.83 and 1.00 respectively. In square hole, centerline effectiveness is less compared to circular hole due to jet lift off and coolant spread more laterally than longitudinally. Results show that as blowing ratio increase effectiveness also increase for fan-shaped hole.

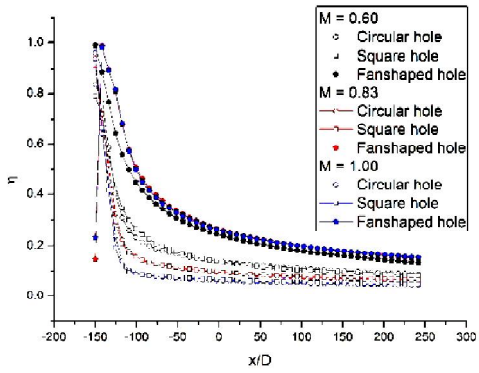

Fig. 8. Centerline Effectiveness for Different Shapes at Different M

Among all the shapes, fan-shaped hole gave the highest effectiveness for all the blowing ratios. It is because of expended exits (exit area is more compared to other hole shapes) in fan-shaped holes. The velocity of coolant from fan-shaped hole exit is less compared to other hole exits as its area increases gradually towards exit causing decrease in coolant velocity. Thus, coolant gets enough time to stay on the plate near the hole exit and hence effective cooling is possible. Therefore, it can be concluded that effectiveness is increased with constant coolant quantity. Coolant inlet volume is constant for all shapes hence the coolant mass required for all shapes is equal and then the comparison is made. The inlet flow conditions were kept constant for all the coolant hole shapes so as to achieve better comparative results.

B. Temperature and Velocity Contours of Different Hole Shapes at Different Blowing Ratios

Figs. (9a-11a) represent temperature contours on lower plate for fan-shaped hole at different blowing ratios. It shows that coolant also flow behind the hole and cool a small area. Near the hole surface, temperature of the hot plate almost reaches 300K. Fig. (9b-11b) represents velocity contours on lower plate for fan-shaped hole at various blowing ratios. Near the hole, there is formation of recirculation zone which spreads laterally and does not affect the path of coolant flow downstream of the holes. As it is clear from the result that coolant flow path is smooth.

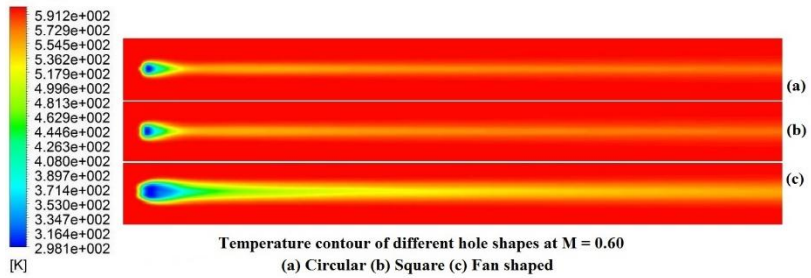

Fig. 9(a). Temperature Contour for M = 0.6

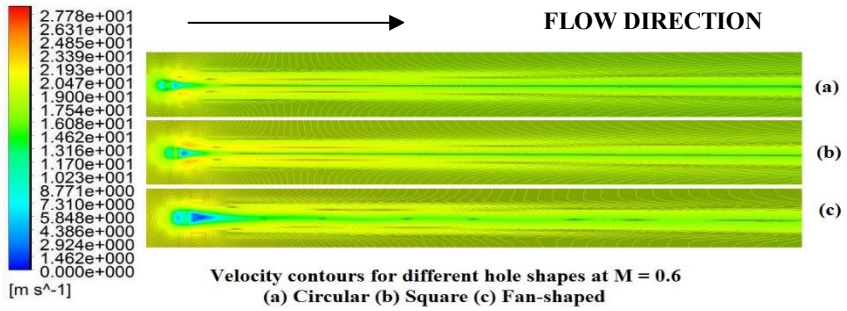

Fig. 9(b). Velocity Contour for M = 0.6

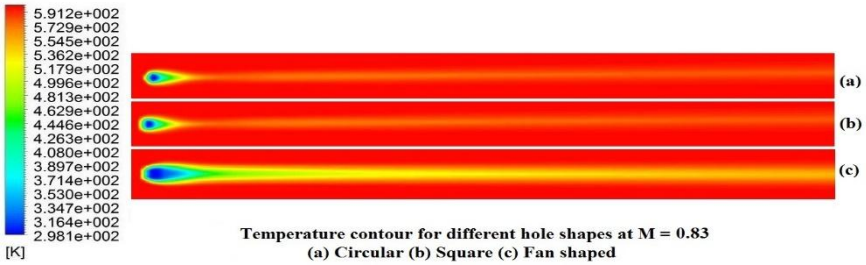

Fig. 10(a). Temperature Contour for M = 0.83

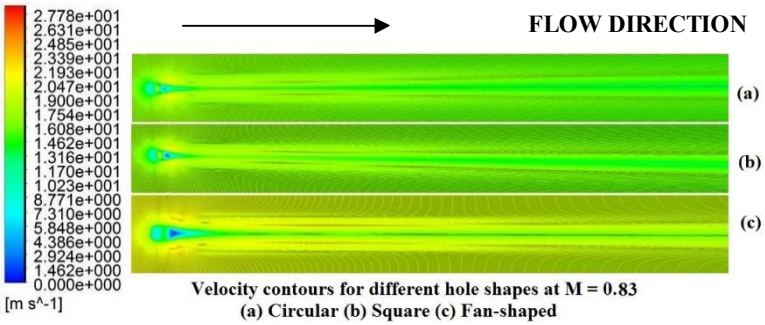

Fig. 10(b). Velocity Contour for M = 0.83

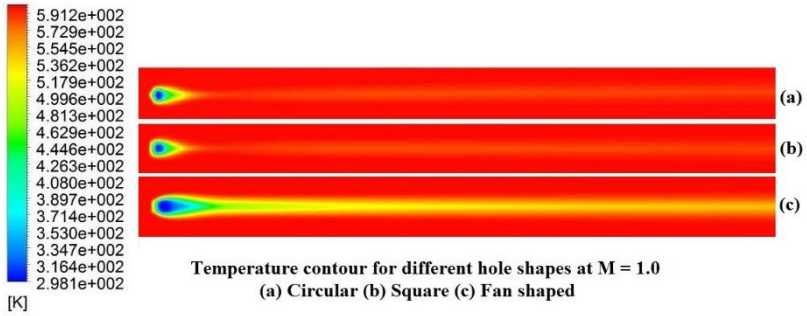

Fig. 11(a). Temperature Contour for M = 1.0

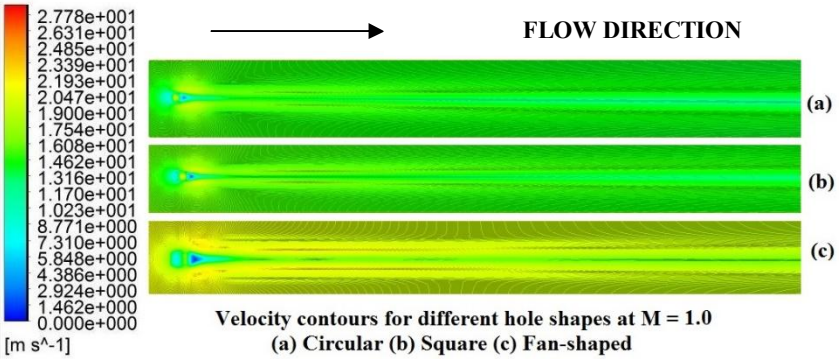

Fig. 11(b). Velocity Contour for M = 1.0

C. *Variation of Spatially Averaged Effectiveness at Different Blowing Ratios (Multiple Holes)*

In order to increase the cooling effectiveness configuration of multiple holes, commonly known as showers were introduced in the plate. Figs. 12-14 show configurations of circular, square and fan-shaped shower.

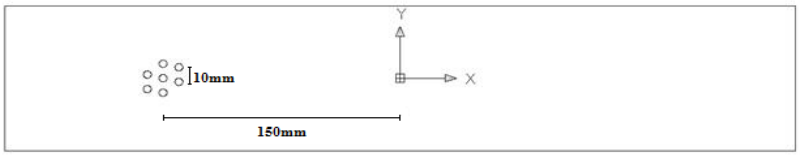

Fig. 12. Configuration for Circular Shower

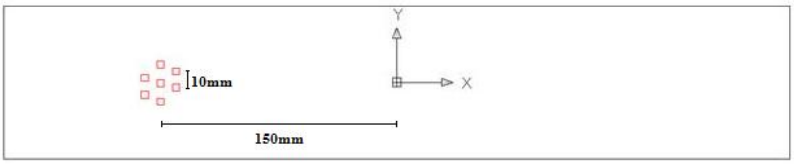

Fig. 13. Configuration for Square Shower

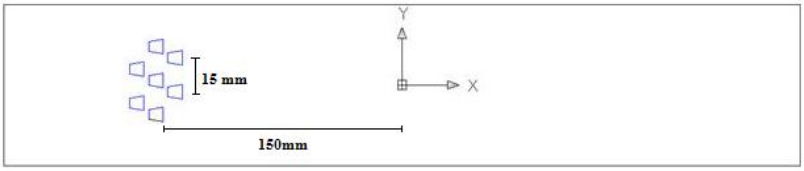

Fig. 14. Configuration for Fan-Shaped Shower

Spatially averaged effectiveness have been compared for circular, square and fan-shaped shower consisting 7 holes for M = 0.60, 0.83 and 1 as shown in Figs. (15-17). From the Figs. (15-17), it is observed that that spatially averaged effectiveness for fan-shaped is higher than square followed by circular because of better lateral spreading of coolant due to expanded exit in fan-shaped holes whereas coolant from circular and square holes is concentrated over a narrow area.

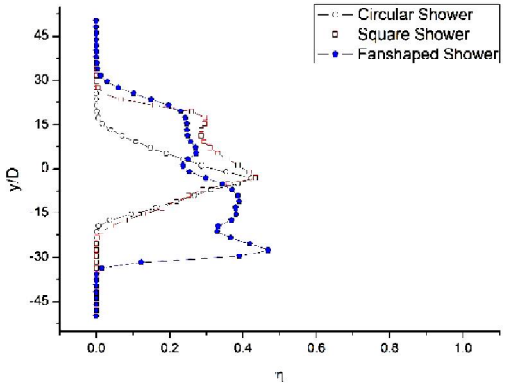

Fig. 15. Spatially Averaged Effectiveness for Shower at M = 0.60

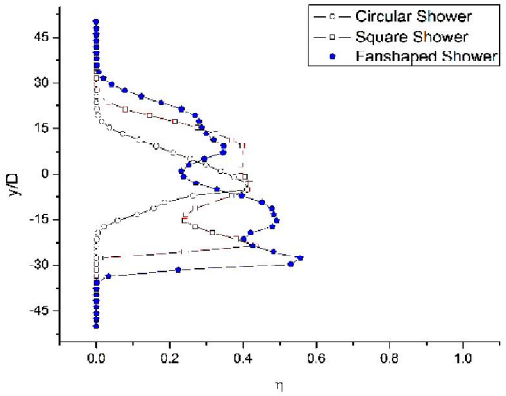

Fig. 16. Spatially Averaged Effectiveness for Shower at M = 0.83

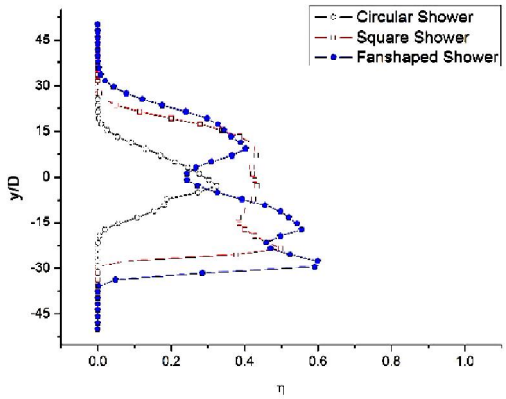

Fig. 17. Spatially Averaged Effectiveness for Shower Arrangement at M = 1.00

From the Figs. (15-17), it is observed that circular shower cool a smaller area of blade surface compared to square and fan-shaped shower. As blowing ratio increase, surface area cooled in lateral and longitudinal direction also increase. These heights signify coolant jet paths whereas depressions signify absence of cooling holes at that position. Hence, it can be concluded that there is zero effectiveness at the mid span between a pair of cooling holes and lower effectiveness at the downstream area due to spreading of coolant. Fig. 18 shows comparison of spatially averaged effectiveness for fan-shaped shower at different blowing ratios. Fig. 19 shows comparison of spatially averaged effectiveness for circular, square and fan-shaped shower at M = 1 at x/D = -100.

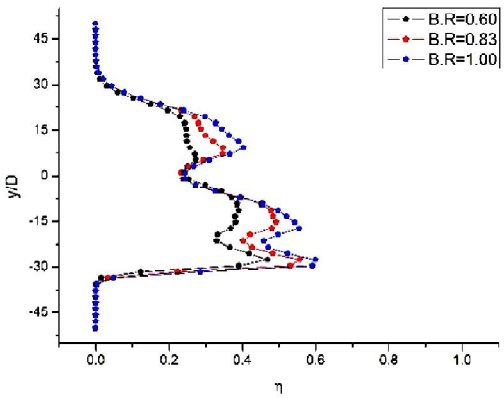

Fig. 18. Spatially Averaged Effectiveness for Fan-Shaped Shower at Different M

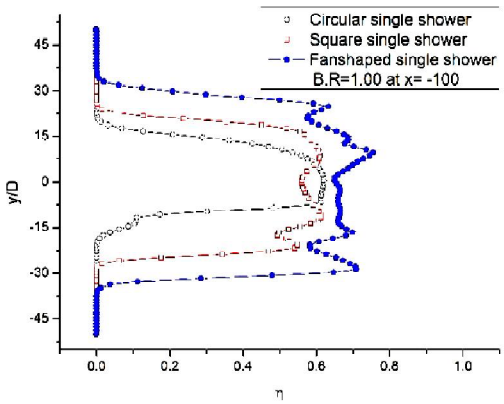

Fig. 19. Spatially Averaged Effectiveness of Shower Arrangement at M = 1 at x/D = -100

From the Fig. 18, it is observed that maximum effectiveness is obtained for fan-shaped hole for blowing ratio equal to 1. It is also observed from Fig. 19 That fan-shaped shower holes are giving higher effectiveness compared to circular and square for same blowing ratio. This result reveal that cooling is effective at a distance of 50 mm downstream of the cooling holes. It will help in determining film cooled length and positioning of next shower or rows of cooling holes on the plate.

Therefore, it can be concluded that effectiveness is higher near the hole region and gradually decrease farther downstream of cooling holes. Thus in fan-shaped shower, coolant spread more laterally as well as longitudinally at M = 1.00 and effectiveness is maximum. Figs. (20-22) show coolant jet height and the spreading of coolant in lateral direction and spanwise direction. In order to capture coolant jet lift off and lateral spreading, the study has been done in three dimensional domain and not in two dimensional domain. It is clear from the results that coolant jet lift off is reduced in fan-shaped hole compared to circular and square hole shapes.

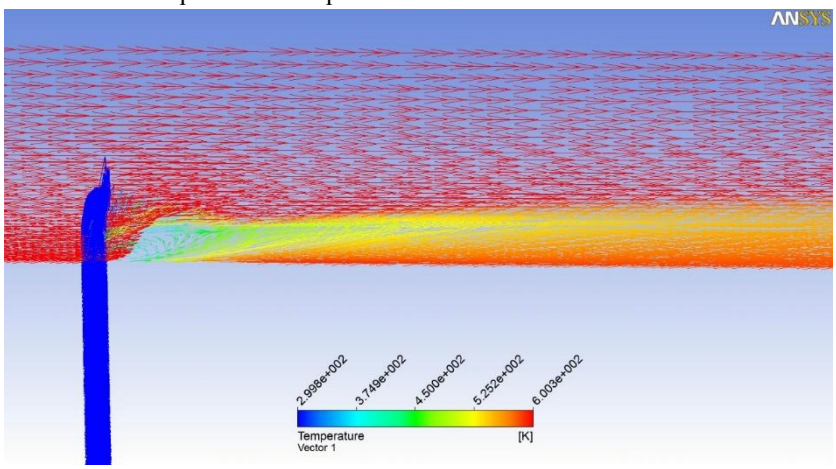

Fig. 20. Jet Heights near Circular Shaped Cooling Hole at M = 1.00

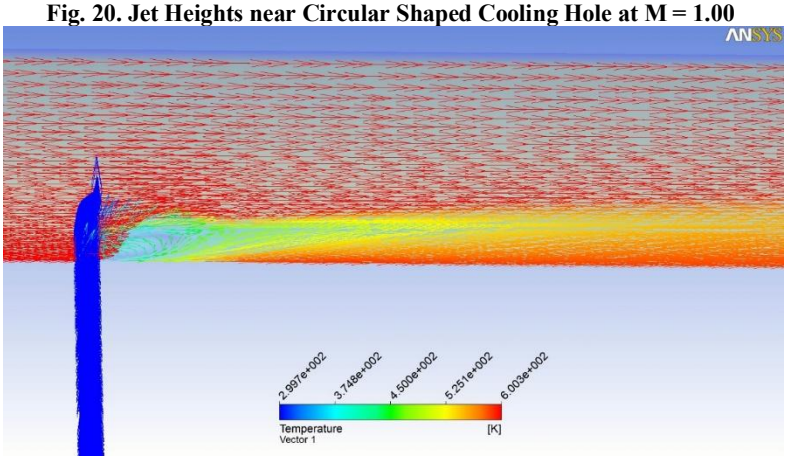

Fig. 21. Jet Heights near Square Shaped Cooling Hole at M = 1.00

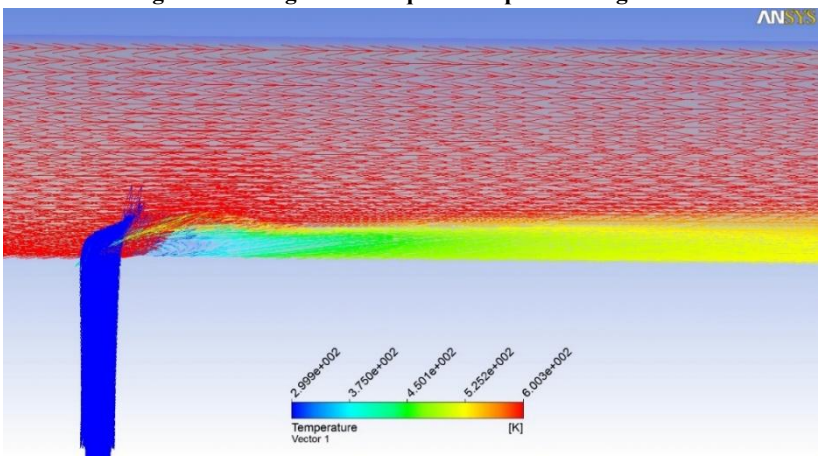

Fig. 22. Jet Heights near Fan-Shaped Cooling Hole at M = 1.00

D. Temperature and Velocity Contours of Shower Holes on Lower Plate at Different Blowing Ratios

The Figs. 23 and 24 show the colour code for the temperature and velocity range. Figs. (25a-33a) represent temperature contours on lower plate for different hole shapes with multiple number of holes at different blowing ratios. It shows that wider area is cooled in case of fan-shaped with same number of holes. Coolant stays on the plate for a larger period of time compared to circular and square hole shapes because of expanded exits. Figs. (25b-33b) represent velocity contours on lower plate for fan-shaped hole at various blowing ratios. Near the hole, there is formation of recirculation zone which spreads laterally. As discussed earlier, the velocity of coolant from fan-shaped hole exit is less compared to other hole exits as its area increases gradually towards exit causing decrease in coolant velocity. Thus, coolant gets enough time to stay on the plate near the hole exit and hence effective cooling is possible.

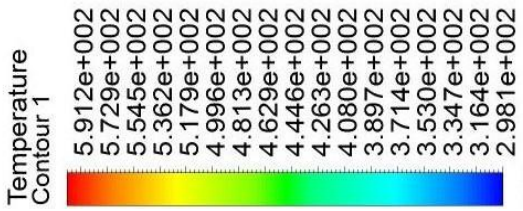

Fig. 23. Range of Temperature for Figs.(25a-33a)

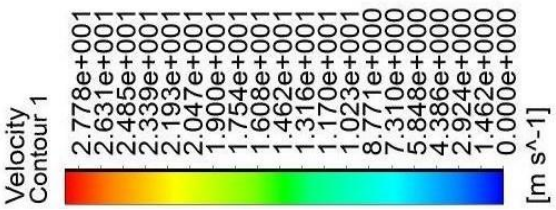

Fig. 24. Range of Velocity for Figs.(25b-33b)

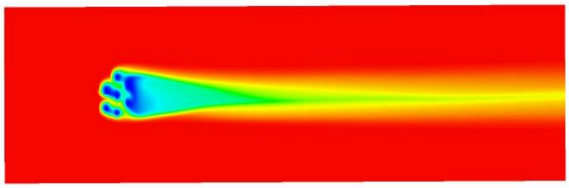

Fig. 25(a). Temperature contour for circular shower at M=0.6

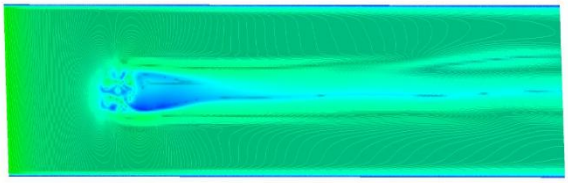

Fig. 25(b). Velocity contour for circular shower at M=0.6

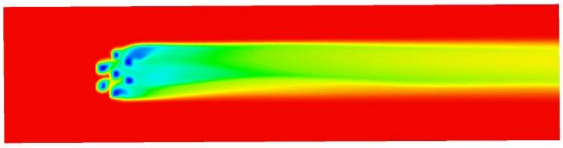

Fig. 26(a). Temperature contour for square shower at M=0.6

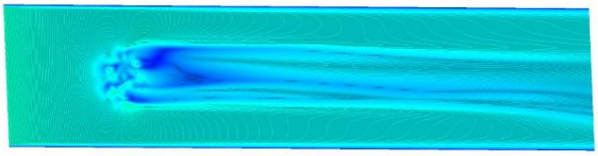

Fig. 26(b). Velocity contour for square shower at M=0.6

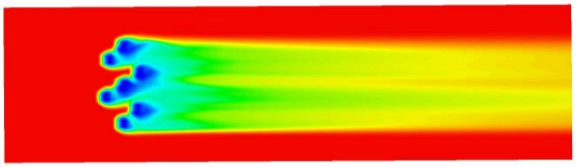

Fig. 27(a). Temperature contour for fan-shaped shower at M=0.6

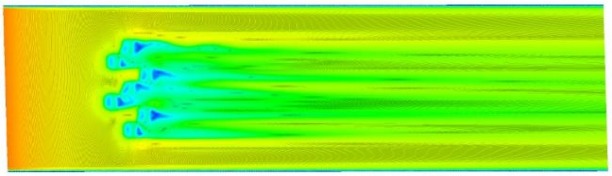

Fig. 27(b). Velocity contour for fan-shaped shower at M=0.6

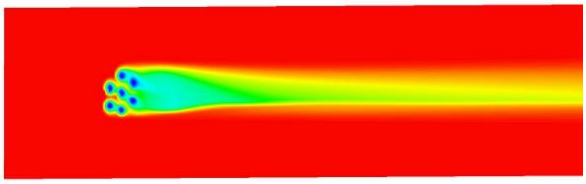

Fig. 28(a). Temperature contour for circular shower at M=0.83

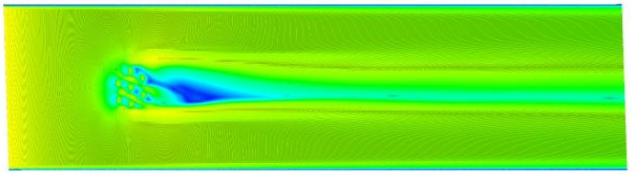

Fig. 28(b). Velocity contour for circular shower at M=0.83

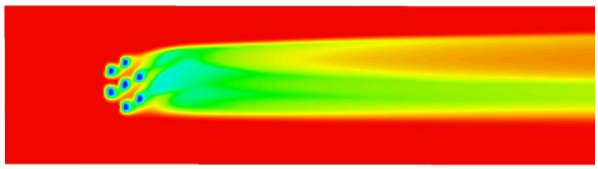

Fig. 29(a). Temperature contour for square shower at M=0.83

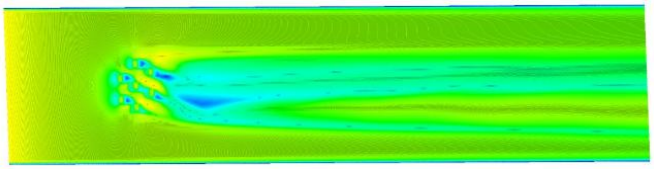

Fig. 29(b). Velocity contour for square shower at M=0.83

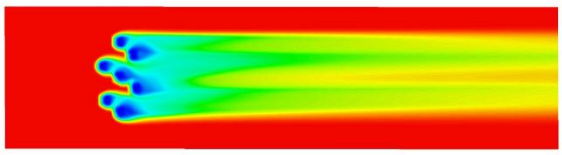

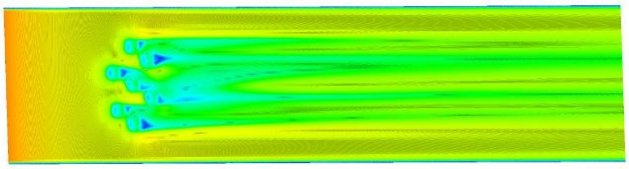

Fig. 30(a). Temperature contour for fan-shaped shower at M=0.83, Fig. 30(b). Velocity contour for fan-shaped shower at M=0.83

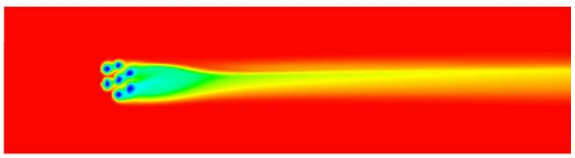

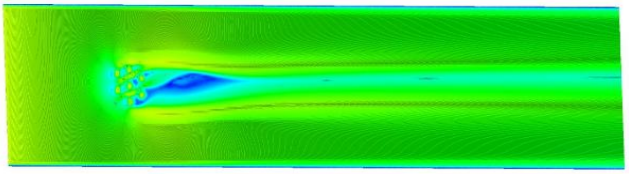

Fig. 31(a).Temperature contour for circular shower at M=1.0, Fig. 31(b).Velocity contour for circular shower at M=1.0

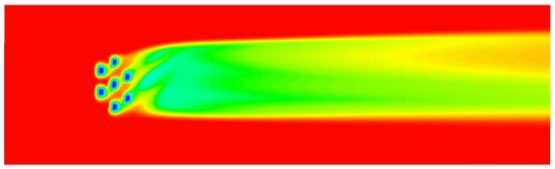

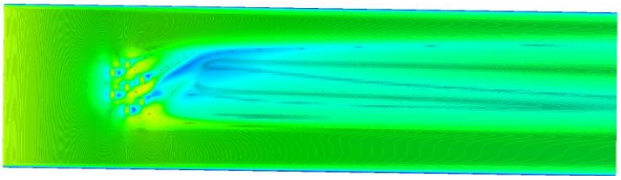

Fig. 32(a). Temperature contour for square shower at M=1.0, Fig. 32(b). Velocity contour for square shower at M=1.0

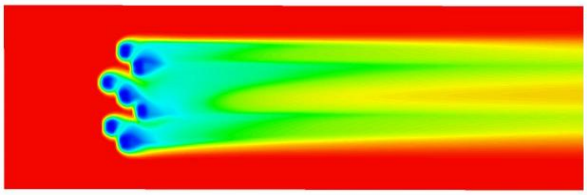

Fig. 33(a). Temperature contour for fan-shaped shower at M=1.00

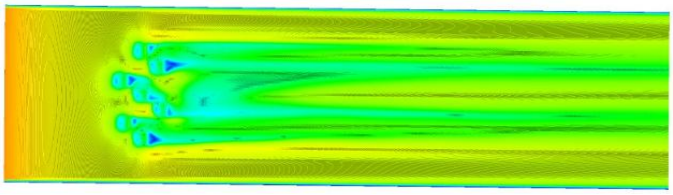

Fig.33 (b). Velocity contour for fan-shaped shower at M=1.00

IV. Conclusion

On comparing centerline effectiveness for single hole, it is observed that effectiveness is very less at the coolant exit for single square hole and fan-shaped hole compared to circular hole due to coolant jet lift off. Then soon effectiveness increases rapidly for fan-shaped hole compared to other two hole shapes because of coolant jet reattachment just downstream of the holes. Effectiveness decrease with increase in blowing ratios for circular and square hole shapes because large proportion of coolant mixes with the mainstream flow rapidly. Spatially averaged effectiveness for fan-shaped is higher than square followed by circular because of better lateral spreading of coolant due to expanded exit, whereas coolant from circular holes is concentrated over a narrow area. Additionally, effectiveness increase with increase in blowing ratio as coolant spread more laterally as well as longitudinally. While for lower blowing ratio, coolant is unable to spread over a longer distance downstream of cooling holes. Thus, best results were obtained for fan-shaped hole with M = 1. Effectiveness of square is less in longitudinal direction compared to circular because of the presence of lateral separation of kidney vortices just downstream of the coolant hole exit. Thus, coolant from square hole spread more laterally than longitudinally. Effectiveness is zero at the mid span between two pair of injection holes and where there is no cooling holes. Hence, it can be concluded that the expanded exit holes (say a fan-shaped one) gives better effectiveness than the conventional hole shapes and can be utilized for more effective cooling of plates with high temperature applications.

References

[1] Mahfoud Kadja and George Bergelest, "Computational study of turbine blade cooling by slot-injection of gas," Applied Thermal Engineering, Vol. 17, No. 12. pp. 1141-1149, 1997.

[2] Michael Gritsch, Achmed Schulz, Sigmar Wittig, "Film cooling holes with expanded exits – Near hole heat transfer coefficients," International Journal Heat and Fluid Flow. 22 134-142, 2001.

[3] Vijay K. Garg, "Modelling of film coolant flow characteristics at the exit of shower head holes," International Journal of Heat and Fluid Flow. 22 134-142, 2001.

[4] Hong Wook Lee, Jung Joon Park, Joon Sik Lee, "Flow visualisation and film cooling effectiveness measurements around shaped holes with compound angle orientations," International Journal Heat and Mass Transfer. 45 145-156, 2002.

[5] C.H.N. Yuen, and R.F. Martinez-Botas, "Film Cooling Characteristics of a Single Round Hole at Various Streamwise Angles in a Crossflow: Part I Effectiveness," International Journal of Heat and Mass Transfer. 46 221-235, 2003.

[6] Joon Ahn, In Sung Jung, Joon Sik Lee, "Film cooling from two rows of holes with opposite orientation angles: injectant behaviour and adiabatic film cooling effectiveness," International Journal Heat and Fluid Flow. 24 91-99, 2003.

[7] James E. Mayhew, James W. Baughn and Aaron R. Byerley, "The effect of free stream turbulence on film cooling adiabatic effectiveness," International Journal Heat and Fluid Flow. 24 669–679, 2003.

[8] Zhi Tao, Zhenming Zhao, Shuiting Ding, Guoqiang Xu, Hongwei Wu, "Suitability of three different two-equation turbulence models in predicting film cooling performance over a rotating blade," International Journal Heat and Mass Transfer. 52 1268-1275, 2008.

[9] W Vickery and H Iacovides, "Computation of gas turbine blade film cooling," Turbulence Mechanics Group, 11th UK National Heat Transfer Conference, 2009.

[10] Sun-Min Kim, Ki-Don Lee and Kwang-Yong Kim, "A comparative analysis of various shaped film-cooling holes," Heat Mass Transfer Springer-Verlag, DOI 10.1007/s00231-012-1043-5, 2012.

[11] Tarek Elnady, Ibrahim Hassan, Lyse Kadem, Terry Lucas, "Cooling effectiveness of shaped film holes for leading edge," Experimental Thermal and Fluid Science 44 649–661, 2013.

[12] Deepak Raj P.Y, Devaraj. K, "Numerical Heat Transfer Analysis of a Flat Plate using Combined Jet Impingement and Film cooling, with Flow Patterns," International Journal of Engineering Research and Technology. ISSN: 2278-0181, Vol. 2 Issue 11, 2013-November.

[13] Vidit Sharma, Ashish Garg, "Numerical investigation of effects of compound angle and length to diameter ratio on adiabatic film cooling effectiveness," ASME, arXiv:1405.0560v1 [cs.CE] 3 May, 2014.

[14] Prakhar Jindal, A.K. Roy, R.P. Sharma, "Numerical Study of film cooling for various coolant inlet geometries," International Journal of Engineering and Technology, ISSN : 0975-4024 Vol 7 No 5 Oct-Nov 2015.